Available online at www.sciencedirect.com

ScienceDirect

Journal of the European Ceramic Society 29 (2009) 2429–2437

www.elsevier.com/locate/jeurceramsoc

Review

Interfacial protonic conduction in ceramics

Hee Jung Park *, Chan Kwak, Kyu Hyoung Lee, Sang Mock Lee, Eun Sung Lee

Samsung Advanced Institute of Technology (SAIT), 14-1 Nongseo-dong, Yongin-si 446-712, Republic of Korea

Received 31 October 2008; received in revised form 9 February 2009; accepted 23 February 2009
Available online 25 March 2009

Abstract

Ceramics displaying protonic conduction have been the subject of intense research due to their potential applications in fuel cells, hydrogen membranes, and water electrolysis equipment. As a result, a number of ceramics presenting high bulk protonic conductivity have been reported; however, overall protonic conductivities in these ceramics are markedly low due to low interfacial conductance. Thus, there has been recent attention to the protonic characteristics in the interface. Interest has greatly increased for nanostructured and heterostructured ceramics using interfacial conductance.

Herein, we summarize the interfacial protonic conductivity and the conduction mechanisms reported in ceramics, with a focus on solid oxides.

Keywords: Interfacial protonic conduction; Nanostructure; Heterostructure; Solid electrolyte; Fuel cells

Contents

1. Introduction

Ionics refers to the field that studies the ionic conduction behavior of materials, rather than electronic conduction behavior. To date, relatively little research has focused on *ionics*, while extensive efforts have been paid to the study of *electronics* due to the increasing development of electronic

---

* Corresponding author. Tel.: +82 31 280 9397.
E-mail address: hj2007.park@samsung.com (H.J. Park).

0955-2219/$ – see front matter © 2009 Elsevier Ltd. All rights reserved.
doi:10.1016/j.jeurceramsoc.2009.02.010

devices.[1,2] In recent years, however, ionic conducting materials for fuel cells and batteries have begun to play an important role due to the increase in energy demand and the environmental crisis.[3–7]

Solid oxide fuel cells (SOFCs) are an environmentally benign power generation method of converting chemical energy into electrical energy. Among the ionic conduction materials, a solid oxide protonic conductor as a solid electrolyte (SE) for SOFCs is a key material to solving the aforementioned problems. Accordingly, a number of materials have been studied extensively, and some protonic conductors such as barium zirconate and barium cerate are prime candidates. For reasons linked to long-term stability and cost, the focus has shifted to the protonic conductors for decreased temperature SOFCs. Decreased temperature, however, requires a decrease of the resistance of ionic transport across the interface (or the grain boundary, gb) dominating the overall resistance of SE. Thus, a fundamental study of the interfacial conduction is crucial to manipulating the overall resistance.[8–13]

Interfacial protonic conduction is even more significant in nanocrystalline materials.[11–13] As the grain size reaches the nanoscale, the portion of gb drastically increases, such that the overall ionic conduction of the nanocrystalline is controlled by electrical charge carrier concentrations and mobilities at the interface.

As described above, the protonic characteristics of the interface are now a very important consideration. However, a summary or review on this topic does not yet exist, while studies on bulk protonic conduction have flourished.[14–16] In this review, we discuss recent studies on the interfacial protonic conduction and the modification of the interfaces of ceramics, primarily solid oxides.

2. General interfacial conduction

2.1. General

Solid oxides are generally polycrystalline forms made up of an assembly of grains (structurally periodicity) joined at the interface of individual grains, termed the gb (Fig. 1). The disruption of the periodicity of the grains in the gb is carried out by strained or missing bonds such that the structure of the gb differs from that of a single grain.

In this polycrystalline material, structural or space charge effects, or both, as an intrinsic conduction mechanism of the gb, have been suggested.[8,12,13,17]

2.2. Structural effect

A crystal structure (e.g., symmetry) is regarded as the most important parameter in ionic motion, which includes both mobility and concentration of ionic charge carriers.[18,19] Accordingly, the structural effects in the gb are readily considered, since uncompensated bonds in the gb core (gbc, Fig. 1a) cause the electrochemical potential of the ions to result in different defects from the bulk ($c_{j,\mathrm{gb}} \gg c_{j,\mathrm{bulk}}$, here j is a charge species, and c, the concentration of j) and offer a more open structure (or excess volume) between the misaligned adjacent grains. Thus, in certain cases, the gb conduction of ionic charge carriers can be greater than the bulk diffusion through the grains.[17,20,21] Wuensch and Tuller reported recently a high mobility of atoms along the gbc in ZnO and observed that structural disorder is accommodated within several atomic planes of the gb.[21–24] Tao and Irvine also reported a similar result in a protonic conductor, showing that the diffusion of the gb is quite fast.[25]

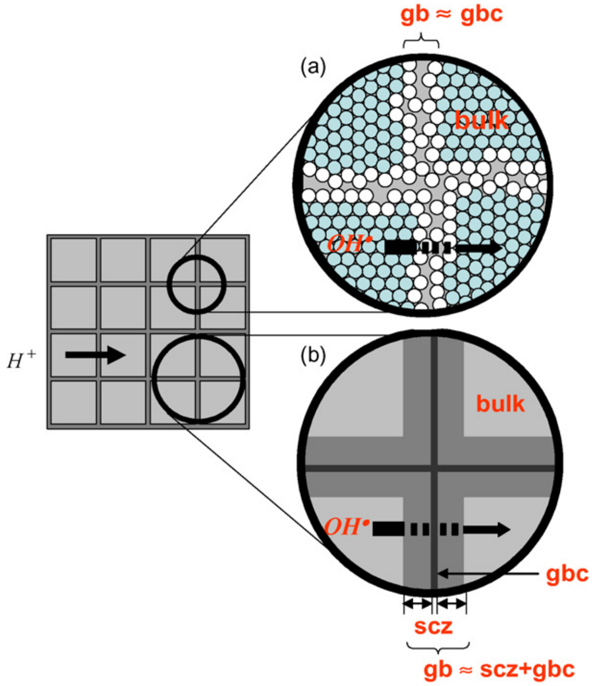

Fig. 1. Schematic diagram of a polycrystalline based on the brick layer model: (a) structural effect and (b) space charge effect on the grain boundary conduction. gb: grain boundary; gbc: grain boundary core; scz: space charge zone.

2.3. Space charge effect

A space charge effect on the gb conduction behavior based on the brick layer model (cubic-shaped grains of identical size having homogeneous grains and gb) has been suggested and theoretically and experimentally examined (Fig. 1b).[12,13] For example, the electrical origin of ionic conduction at the gb of oxides such as zirconias, cerias, lanthanum gallates, and halides has been intensively studied.[12,13,26,27] As a result, it is proven that the ionic charge carrier depletes and accumulates in the vicinity (space charge zone, scz, Fig. 1b) of the gbc that structurally differs from the bulk. In the space charge effect, such a depletion or accumulation of charge carriers is attributed to the existence of excess charge in the gbc, which is inevitably formed due to thermodynamic differences between the gbc and bulk.[28–30] Consequently, the concentration of the charge carriers markedly modified at the scz affects the gb conductance.

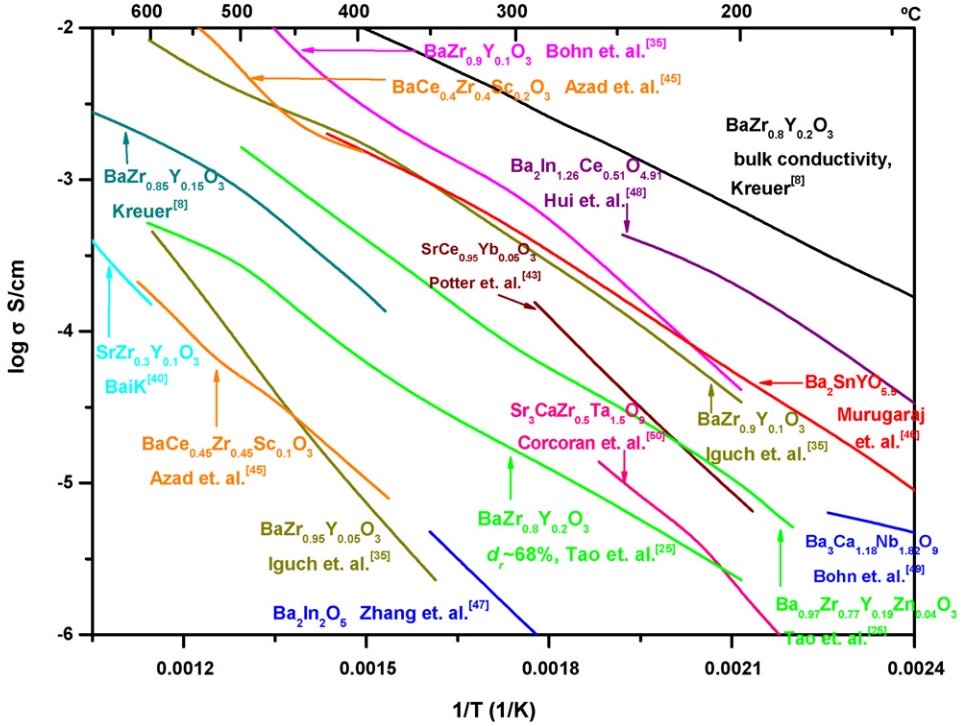

Fig. 2. The grain boundary conductivities in well-known protonic conductors under wet atmosphere are compared as functions of temperature. As a reference, the bulk estimated conductivity in $BaZr_{0.8}Y_{0.2}O_{3-\delta}$ is also plotted.

3. Interfacial protonic conduction of perovskites and related structures

3.1. Interfacial protonic conductivity

After protonic conduction in a ceramic was first introduced by Stotz and Wagner at high temperatures,[31] research of ceramics has intensified. Among those materials, perovskites (ABO_3) and related materials have received great attention due to their very high protonic conductivity.[8,32–34] In Fig. 2, the gb conductivities (σ_{gb}) reported in those materials are plotted as functions of temperature (they are also summarized in Table 1).

3.1.1. Interfacial protonic conductivity of perovskites

Among perovskites, barium zirconates are particularly appealing candidates for the protonic solid-electrolyte of fuel cells because they have the highest protonic conductivity of the bulk.[8,35,36] As a reference, the protonic conductivity of bulk (σ_{bulk}) $BaZr_{0.8}Y_{0.2}O_{3-\delta}$ estimated from Kreuer's data was plotted.[8] Its gb conductivities, however, are not as high as that of the bulk, as seen in Fig. 2.

Iguch et al. made a high density sample of $BaZr_{0.9}Y_{0.1}O_{3-\delta}$ (BZY, relative density, $d_r > 97\%$) to precisely examine the gb conduction.[35] As a result, they observed that it is, in fact, lower than that of the bulk ($\sigma_{bulk} \sim 3 \times 10^{-3}$ S/cm and $\sigma_{gb} \sim 4 \times 10^{-4}$ S/cm at 300 °C), and the activation energy of the gb ($E_{gb} \sim 0.5$ eV at 200–400 °C) is higher than that of the bulk ($E_{bulk} \sim 0.4$ eV in 100–400 °C), showing that the overall conductivity of barium zirconates must be determined by the gb conductivity as temperature decreases.[35–39] They also computed the specific gb conductivity (a single gb conductivity, $\sigma_{gb}^{sp} = \sigma_{bulk} \cdot (\tau_{bulk}/\tau_{gb})$, here $\tau = RC$, resistance and capacitance) from the resistances and capacitances as a function of Y-doping concentration. It is approximately three orders of magnitude lower than that of the bulk. For instance, σ_{gb}^{sp} of $BaZr_{0.95}Y_{0.05}O_{3-\delta}$, $BaZr_{0.90}Y_{0.10}O_{3-\delta}$, and $BaZr_{0.85}Y_{0.15}O_{3-\delta}$ were $\sim 3 \times 10^{-8}$ S/cm, 4×10^{-7} S/cm, and 2×10^{-6} S/cm at 300 °C, respectively.

Tao and Irvine studied the gb conduction of BZY with ZnO. By adding ZnO, the relative density of the sample increased by 28% (its d_rs are 68% and 96%, respectively, when sintered at 1325 °C). The gb conductivity increased by one order of magnitude in the high density sample, as seen in Fig. 2.[25]

Zirconates having different atoms at the A-site of ABO_3 (in $AZrO_3$, A = Sr, Ca) have also been studied intensively, but they do not appear to be as potentially attractive as barium zirconates due to their low protonic conductivities.[16,19,40] As an example, the gb conductivity of $SrZr_{0.9}Y_{0.1}O_{3-\delta}$ presented by Baik is plotted in Fig. 2.[40]

Another important class is barium cerates due to their comparable protonic conductivities with barium zirconates. Kreuer reported a semicircular impedance pattern corresponding to the gb in $BaCe_{0.9}Y_{0.1}O_{3-\delta}$ (BCY), which is significantly smaller than that of BZY at 100 °C under wet atmosphere. This indicates that the Ce ion, rather than the Zr ion, at the B-site of the perovskite may be preferable in view of the gb conduction.[18] However, it is questionable whether it comes from an intrinsic effect since the relative density of BZY is low (~91%) compared to that of BCY (~98%).[18,32,41] This point was clarified by Haile et al. by preparing clean and high-density (>95%) samples. They examined the protonic conduction of $BaCe_{0.9-x}Zr_xGd_{0.1}O_{3-\delta}$ and $BaCe_{0.9-x}Zr_xNd_{0.1}O_{3-\delta}$ as a function of Zr-content ($x = 0$,

Table 1
Comparisons of the grain boundary conductivities in the protonic conductors.

Materials	Sintering temperature (°C)	d_r (%)	gb conductivity (S/cm)	Temperature (°C)	Atmosphere
$BaZr_{0.9}Y_{0.1}O_3$[9]	1700	>95	$\sim 2 \times 10^{-3}$	600	Wet (1.7%)-H_2
$BaZr_{0.9}Y_{0.1}O_3$[36]	1715	97	$\sim 4 \times 10^{-5}$	200	Wet (10%)-Ar-O_2
$BaZr_{0.9}Y_{0.1}O_3$[35]	1800	–	$\sim 3 \times 10^{-4}$	300	Wet (2.3%)-air
$BaZr_{0.85}Y_{0.15}O_3$[8]	1700	90	$\sim 2 \times 10^{-4}$	400	Wet (2.3%)-N_2
$BaZr_{0.8}Y_{0.2}O_3$[8]	1700	92	$\sim 10^{-3}$	400	Wet (2.3%)-N_2
$BaZr_{0.8}Y_{0.2}O_3$[25]	1325	68	$\sim 3 \times 10^{-6}$	250	Wet-5% H_2-Ar
$Ba_{0.97}Zr_{0.77}Y_{0.19}Zn_{0.04}O_3$[25]	1325	96	$\sim 3 \times 10^{-5}$	250	Wet-5% H_2-Ar
$SrZr_{0.9}Y_{0.1}O_3$[40]	1600	–	$\sim 2 \times 10^{-4}$	600	Wet-Ar
$BaCe_{0.9}Y_{0.1}O_3$[84]	1550	92	$\sim 2 \times 10^{-3}$	275	Wet-H_2-Ar
$BaCe_{0.9}Y_{0.1}O_3$[18]	>1700	>98	$\sim 2 \times 10^{-6}$	100	Wet (2.3%)-N_2
$BaCe_{0.75}Y_{0.25}O_3$[83]	1450	95	$10^{-3 \text{ to } 4}$	300	Wet-H_2-Ar
$BaCe_{0.9}Gd_{0.1}O_3$[42]	1550	>95	$\sim 10^{-4}$	200	Wet-Ar
$BaCe_{0.8}Zr_{0.1}Nd_{0.1}O_3$[42]	1650	>95	$\sim 10^{-3\text{–}4}$	250	Wet-Ar
$BaCe_{0.8}Zr_{0.1}Gd_{0.1}O_3$[42]	1550	>95	$\sim 10^{-3\text{–}4}$	250	Wet-Ar
$Ba(Y_{0.15}Zr_{0.807}Ce_{0.043})O_3$[8]	–	–	$\sim 2 \times 10^{-3}$	400	Wet (2.3%)-N_2
$BaCe_{0.45}Zr_{0.45}Sc_{0.1}O_3$[45]	1600	75	$\sim 10^{-5}$	400	Wet (3%)-H_2-Ar
$SrCe_{0.95}Yb_{0.05}O_3$[43]	1500	92	$\sim 2 \times 10^{-4}$	300	Wet-Ar
$La_{0.6}Ba_{0.4}ScO_3$[84]	1600	–	$\sim 10^{-4}$	300	Wet (6.1%)-N_2
$Ba_2YSnO_{5.5}$[46]	1600–1700	85–95	$\sim 5 \times 10^{-4}$	300	Wet (2.3%)-N_2
$Ba_2In_{1.26}Ce_{0.51}O_{4.91}$[47]	1250	93	$10^{-3 \text{ to } 4}$	200	Wet-N_2
1/3($Ba_3Ca_{1.17}N_{b1.83}O_9$)[18]	>1700	>98	$\sim 2 \times 10^{-6}$	100	Wet (2.3%)-N_2
$Ba_3Ca_{1.18}Nb_{1.82}O_9$[49]	1600	96–98	$\sim 7 \times 10^{-6}$	170	Wet-Ar-O_2
$Sr_3CaZr_{0.5}Ta_{1.5}O_9$[50]	1430	90	$\sim 7 \times 10^{-5}$	300	Wet-H_2-Ar
nano-$BaZr_{0.8}Y_{0.2}O_3$[8]	–	–	$\sim 5 \times 10^{-6}$	400	Wet (2.3%)-N_2
nano-$BaZr_{0.8}Y_{0.2}O_3$[10]	800	90.3	$\sim 1 \times 10^{-7}$	300	Wet (2.5%)-Ar
nano-$BaZr_{0.8}Y_{0.2}O_3$[10]	1250	98.1	$\sim 1 \times 10^{-4}$	300	Wet (2.5%)-Ar
nano-$BaCe_{0.5}Zr_{0.4}Y_{0.1}O_3$[63]	1650	>95	$\sim 1 \times 10^{-4}$	400	Dry-H_2

nano: Nanostructure.

0.1, and 0.2) and calculated the specific gb conductivities to determine the Zr-effect on the gb. As a result, the conductivities with $x = 0, 0.1$, and 0.2 were $\sim 3 \times 10^{-6}$ S/cm, $\sim 7 \times 10^{-7}$ S/cm, and $\sim 2 \times 10^{-7}$ S/cm, respectively, at 300 °C.[59] It clearly shows that the addition of Zr at the B-site of ABO_3 decreases the gb conductivity. They also studied the dependence of Gd-content and displayed that the higher the Gd-doping concentration is, the higher the gb conductivity is. For example, σ_{gb}^{sp} of $BaCe_{0.9}Gd_{0.1}O_{3-\delta}$ and $BaCe_{0.85}Gd_{0.15}O_{3-\delta}$ were $\sim 3 \times 10^{-6}$ S/cm and $\sim 2 \times 10^{-5}$ S/cm, respectively, at 300 °C.[42]

Cerates, like zirconates, have been modified by changing the Ba ion of the A-site to Sr or Ca. However, the results are not as good as those of barium cerates.[43,44] As an example, the gb conductivity of $SrCe_{0.95}Yb_{0.05}O_{3-\delta}$ is shown in Fig. 2.[42]

$BaCe_{0.4}Zr_{0.4}Sc_{0.2}O_{3-\delta}$ and $BaCe_{0.45}Zr_{0.45}Sc_{0.1}O_{3-\delta}$ doped with a 1:1 ratio of Ce and Zr at the B-site as rather complicated forms were studied by Azad and Irvine.[45] The gb conductivity of the high-doping case ($BaCe_{0.4}Zr_{0.4}Sc_{0.2}O_{3-\delta}$) is similar to that of BZY, but that of the low doping severely decreases, as evident from Fig. 2.

3.1.2. Interfacial protonic conductivity of perovskite-related materials

Some of the perovskite materials are known to have high protonic conductivity, as seen above, but they are still not used commercially; thus, the search for materials with higher protonic conductivity continues. In recent years, researches into perovskite-related materials have increased, since they can take advantage of perovskites showing high ionic mobility, as well as offer more ionic defects, implying the possibility for high concentrations of the protonic defects.[46,47] One such structure is a brownmillerite with double unit cell formed by the ordering of B-site cations. In the following, the gb protonic conductivities of some brownmillerites are given.

Murugaraj et al. reported that $Ba_2YSnO_{5.5}$ shows high bulk protonic conductivity, while the gb shows low protonic conductivity due to both extrinsic effects (amorphous phases) and intrinsic effects (structural instability).[45] However, when compared to other materials of Fig. 2, its gb conductivity is acceptable at the investigated temperature range. Zhang and Smyth reported the gb conductivity of $Ba_2In_2O_5$, another material with the same structure. As seen in Fig. 2, it is very low. As an example, σ_{gb} is about 10^{-6} S/cm at 300 °C (note that it is about 10^{-3} S/cm in BZY).[47] Hui et al. prepared Ce-doped $Ba_2In_2O_5$ (BIC) with hot press sintering (1250 °C/150 MPa) and reported that its electrical property is very sensitive to the presence of hydrogen at 100–250 °C, that is, to the existence of the proton conductivity.[48] Its gb proton conductivity is the highest among the materials compared at low temperature (100–250 °C), as seen in Fig. 2.

Complex perovskites of the form $A(B'_{1/3}B''_{2/3})O_{3-\delta}$ or $A_3(B'B'')O_{9-\delta}$ have also become of interest due to their comparable protonic conductivities with barium zirconates.[18,49–51] Bohn et al. reported that, in $Ba_3Ca_{1.18}Nb_{1.82}O_{9-\delta}$ (BCN18) prepared by conventional ceramic processing, no gb protonic conduction is observed, but for BCN18 prepared by sol–gel processing, it is observed, implying that gb protonic conduction depends on the nature of the powder processing.[49] The gb conductivities of BCN18 are plotted in Fig. 2.

The gb conductivity of $Sr_3CaZr_{0.5}Ta_{1.5}O_{9-\delta}$, a more complicated material, was also examined by Corcoran and Irvine and is shown in Fig. 2.[50] Savanju and Irvine studied the gb conductivity of $Sr_3Ca_{0.95}Zn_{0.05}Zr_{0.5}Ta_{1.5}O_{9-\delta}$ and $Sr_3Ca_{0.9}Zn_{0.1}Zr_{0.5}Ta_{1.5}O_{9-\delta}$ and determined that higher conductivity results from high doping with Zn.[51]

Other protonic conductors having pyrochlore and fluorite structures have also been reported,[52–54] but their gb conductions have not been fully elucidated.

3.2. Interfacial protonic conduction mechanism

3.2.1. Structural effect of the protonic conduction

The interfacial conduction mechanism of protons is difficult to fully describe since the gb conduction depends on a number of disparate factors, including relative density, glassy phase (CaO, SiO_2, etc.), impurities, crystal structure, microstructure, and charge species.[55,56] Accordingly, the gb conductivity can differ due to varying material processing even though the composition of the material is similar. Nevertheless, the cause of the gb resistance (i.e., the structural distortion or space charge being able to affect the gb resistance) in highly pure and dense samples has been of great interest, specifically as a blocking source for protonic transfer.

Kreuer et al. have reported low gb conductance in perovskites, as seen in Fig. 2.[8] They suggested that the gbc is responsible for the low conductivity since they believe that structural distortions in the gbc most likely lead to a decrease of protonic mobility and a depletion of protonic defects (see Fig. 1a).[8,10] Their suggestion for the protonic motion is that the proton strongly interacts with the valence electron density of the nearest neighbor, making a strong bonding interaction with the nearest oxygen (O–H) and a weak bonding interaction with the next-nearest oxygen (O···H). For example, in barium zirconate, the distance of the strong bonding interaction is <100 pm, while that of the weak bonding interaction is 250–280 pm, forming O–H···O (hydrogen bonding). According to their suggestion, the energy of the hydrogen bonding is compensated by the BO_6-octahedral structural energy and this compensation leads to the strong fluctuations of the hydrogen bonding length for proton conduction. They also observed that high mobility in $SrTiO_3$ and $CaTiO_3$ is related to a small lattice parameter as a structural effect.[8,57,58]

Shi et al. similarly highlighted the importance of the structure for proton transfer.[19] They mentioned that In-doped $CaZrO_3$ or $SrZrO_3$, with an orthorhombic structure has a unique stabilized proton site located between two adjacent octahedrals. However, In-doped $BaZrO_3$, a cubic structure, bears a specific region of stable sites between them. That is, when the cubic structure changes to orthorhombic, ZrO_6 octahedra rotate, causing an increase in the activation energy of the protonic conduction. Consequently, barium zirconate shows better gb conductivity than calcium and strontium zirconates.

3.2.2. Space charge effect of the protonic conduction

From a totally different point of view have some researchers suggested that the space charge effect may serve as a blocking source for the gb protonic conduction. That is, a protonic charge carrier with a positive valence could deplete in the vicinity of the gbc due to the positive space charge potential. Iguchi et al. fabricated highly dense and clean barium zirconates using a solid state reaction method by sintering at 1800 °C for 20 h. Their goal was to elucidate the space charge or structural effect on the conduction of the protonic charge carrier through the gb.[35] They tested the gb conductivity as a function of dopant concentration (5–15% Y) and observed that it increases by approximately three orders of magnitude as the Y-concentration increases. They suggested the space charge effect as a possible resistance mechanism, since the gb resistance could not be explained by a structural effect such as the differences between the average grain diameters, gb character distributions, or secondary phases.

Bohn et al. also proposed that the gb conduction in BCN18 may be controlled by the depletion of positively charged defects at the scz, pointing out that the electrical gb thickness composed of the gbc and scz is ~4 nm (note that the thickness of the gbc is generally ~1 nm).[49]

3.2.3. Other effects of the protonic conduction

Ryu and Haile suggested another conduction mechanism of the gb. They examined the gb conduction of barium cerate and zirconate solid solutions doped with Gd or Nd and showed that the activation energy of the gb tends to increase with decreasing the doping concentration as well as unit cell volume.[42] By doing so, they believed that the gb conduction is controlled not only by the unit cell volume but also by the basicity of the metal oxide component, the polarizability of the cation, and the association of the dopant hydroxyl group.

4. Interfacial protonic conduction of nanostructured materials

Great efforts have been devoted to search a protonic conductor with high protonic conductivity. In recent years, as a way to identify the protonic conductors having high protonic conductivity, nanostructured materials have been employed. This approach has been carried out in other research areas dealing with oxygen ionic conduction, and it was discovered that the oxygen ionic conductivity is in certain cases enhanced by nanostructures.[59–62] To date, however, there has been no reported enhancement among the protonic conductors.[8,10,47] As seen in Fig. 3, Cerversa et al. have studied the protonic conduction of $BaZr_{0.8}Y_{0.2}O_{3-\delta}$ which bears defined nanostructures (average grain sizes are ~10 nm, ~50 nm, and ~200 nm), and they have reported a negative effect on the overall conduction (for comparison, the bulk conductivity of $BaZr_{0.8}Y_{0.2}O_{3-\delta}$ reported by Kreuer was inserted). Particularly, the overall conductivity in the 10 nm sample drastically decreased.[10] For example, σ_{gb} of the 10 nm sample is $\sim 10^{-6}$ S/cm, while σ_{gb} of the 200 nm sample is $\sim 10^{-3}$ S/cm at 400 °C. Kreuer also prepared a thin film of $BaZr_{0.8}Y_{0.2}O_{3-\delta}$ having a nanos-

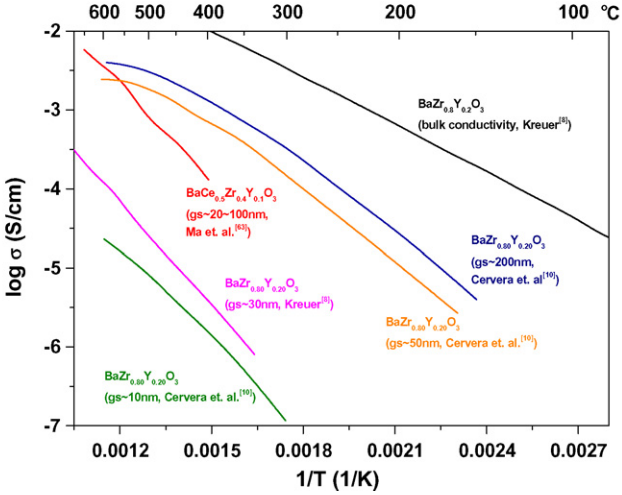

Fig. 3. The protonic conductivities of nanostructured protonic conductors are plotted as functions of temperature. As a reference, the bulk estimated conductivity in $BaZr_{0.8}Y_{0.2}O_{3-\delta}$ is also plotted.[8] gs is the grain size.

tructure (grain size ∼30 nm), which also showed very low conductivity.[8] Ma et al. fabricated nanostructured barium cerate-based film ($BaCe_{0.5}Zr_{0.4}Y_{0.1}O_{3-\delta}$) from nano-grain feedstock using an air plasma spray.[63] As seen in Fig. 3, its protonic conductivity was nearly as low as those of other nanostructures.

In spite of this negative effect, nanostructures are still considered to be potential sources for modified conductivity. As a good example, it was reported very recently that fluorite materials known to be oxygen ionic conductors show protonic conduction in nanostructures. Guo first attempted to determine whether there was a water effect on conduction by making a nanostructure with yttria stabilized zirconia (YSZ) film, a famous oxygen ionic conductor, and reported that protonic defects were found to form on the surface and diffuse along the gb into the interior of the specimen in boiling water.[64] Anselmi-Tamburini et al. also measured the protonic conduction in highly dense nanostructured YSZ with a grain size of ∼15 nm, made by spark plasma sintering (SPS) at low temperature.[65] Park and Kim confirmed this result by first making a water concentration cell operating at room temperature.[66] They showed that an equilibrium potential (or OCV) as high as ∼0.4 V in SDC (Sm-doped CeO_2) is produced by introducing wet air into the cell while the outside is immersed in water, verifying the protonic conduction in nanostructured fluorites. They also demonstrated that a short circuit current is only produced in nanostructures. That is, no current was detected in microstructured fluorites. In the view of conduction mechanism, this strongly suggests that the protonic charge carrier goes through the sample along the gb, even though the exact mechanism is not discussed or postulated.

One possible mechanism of the protonic conduction along the gb in nanostructured fluorites involves water passing into the gb which has a large open space (a free volume) by physisorption and chemisorption reactions (see Fig. 4). Similarly, Raz et al. reported the protonic conduction in porous-YSZ with a surface-conduction mechanism.[67] They demonstrated that the physisorption reaction dominantly takes place at low temperatures (<100 °C), and the chemisorption reaction dominantly takes place at high temperatures (>100 °C), as shown in Fig. 4. This behavior has been reported in many metal oxides, including Al_2O_3, TiO_2, SiO_2, and α-Fe_2O_3, by forming single or multi-observed water layers.[68–70] Anderson and Parks explained in detail that the protonic conduction on silica surfaces is due to adsorption isotherms that are formed by freely vibrating hydroxyl groups offering the strongest surface adsorption sites.[70] Yamada et al. also suggested the surface conduction mechanism by adsorption of water in a one-dimensional nanostructure ($H_2Ti_3O_7$ nanotube).[11]

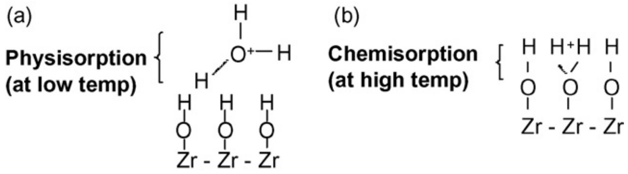

Fig. 4. Schematic diagram of (a) physisorption reaction and (b) chemisorption reaction on zirconia surface.[67]

As another possible conduction mechanism, a layer conduction transfer between unit cells can be taken into account. This behavior has often been shown in materials having a layer structure by containing water itself, such as $WO_3 \cdot n(H_2O)$ and $MoO_3 \cdot 2H_2O$.[71,72]

5. Interfacial conduction of heterostructured materials

Many groups have studied heterogeneous nanomaterials using the surface conducting pathway in an attempt to modify ionic conductivity.[26,73–76] As a result, some heterogeneous nanostructured materials showing an enhancement in conductivity have been discovered in several ionic conductors.

The first approach taken was an enhancement of Li-ionic conductivity, achieved by adding nanosized alumina, an inert particle, into LiI.[73] In this system, the conductivity increases by orders of magnitude and is highly dependent on the interfacial area between the host and inert particles. After this seminal discovery, many heterogeneous composites have followed, and some of them have shown a positive conductive effect.[74–76] This behavior has even been demonstrated in bilayer thin films without adding inert oxide particles.[77] Sata et al. made a bilayer thin film system of BaF_2/CaF_2 having F-ionic conduction and showed that the thinner each layer was, the higher the degree of conductivity of the thin film. In some cases, the overall conductivity increased by up to two orders of magnitude. Maier suggested that this improvement was a result of the space charge effect enhancing the concentration of the charge carrier in the vicinity of the interface between the two different phases of the scz.[26] This behavior has also been reported for materials known to be oxygen ionic conductors, including bilayer thin films of ZrO_2 and GDC (Gd-doped CeO_2).[78] However, the authors suggested that the enhanced conductivity is not attributed to the space charge effect. They mentioned that it may result from either dopant solubility or an increase of the oxygen vacancy

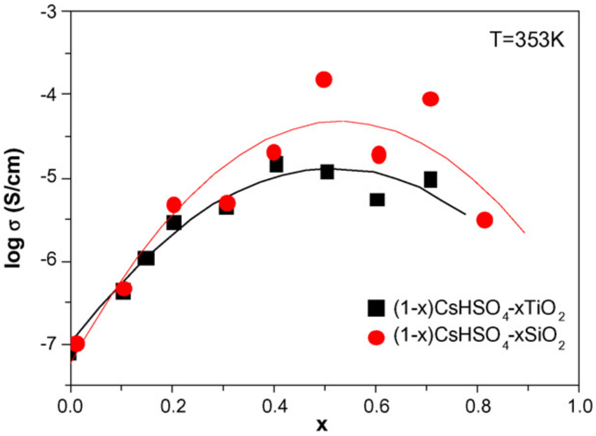

Fig. 5. The protonic conduction behavior depending on the concentration of inert species in the heterostructure (matrix: $CsHSO_4$, and inert species: TiO_2 and SiO_2).[79–82].

mobility caused by strain enhancement at the interface of the ZrO_2 and GDC layers.

Similarly, in protonic conductors such as sulfate and phosphate systems, heterostructures have been studied. As shown in Fig. 5, finely dispersed oxides (TiO_2 and SiO_2) in the host matrix (sulfates) increase the protonic conductivity by orders of magnitude.[79–82] Ponomareva et al. believed that the enhanced conductivity may be due to the space charge effect, showing that the conductivity depends on the dispersoid concentration and specific interface area between two phases.

As mentioned above, heterostructures show a positive effect on ionic conduction, but the cause of the enhancement is still controversial. It is, however, certain that heterostructures have a high potential for being able to manipulate the interfacial protonic conduction and, furthermore, for maximizing the overall protonic conductivity.

6. Concluding remarks

A number of ceramics showing high bulk protonic conductivities have been reported, but their gb protonic conductivities are markedly low. This has spurred research into improved gb conduction. In addition, attention is also shifting toward interface-modified materials. In the current paper, we have reviewed the interfacial protonic conduction in ceramics, mainly solid oxides, including nanostructures and heterostructures. The conduction mechanisms of the interface, as well as the structural and space charge effects, were highlighted.

References

1. Hosono, H., Recent progress in transparent oxide semiconductors: materials and device application. *Thin Solid Films*, 2007, **515**, 6000.
2. Shur, M. S., Gaska, R. and Bykhovski, A., GaN-based electronic devices. *Solid-State Electron.*, 1999, **43**, 1451.
3. Yamamoto, O., Solid oxide fuel cells: fundamental aspects and prospects. *Electrochim. Acta*, 2000, **45**, 2423.
4. Zhang, F., Chan, S. W., Spanier, J. E., Apak, E., Jin, Q., Robinson, R. D. *et al.*, Cerium oxide nanoparticles: size-selective formation and structure analysis. *Appl. Phys. Lett.*, 2002, **80**, 127.
5. Park, H. J. and Kim, S., Electrochemical characteristics of ZnO-nanowire/yttria-stabilized zirconia composite as a cathode for solid oxide fuel cells. *Electrochem. Solid-State Lett.*, 2007, **10**(11), B187.
6. Park, H. J. and Choi, G. M., The electrical conductivity and oxygen permeation of ceria with alumina addition at high temperature. *Solid State Ionics*, 1746, **2008**(178).
7. Hino, R., Haga, K., Aita, H. and Sekita, K., R&D on hydrogen production by high-temperature electrolysis of steam. *Nucl. Eng. Des.*, 2004, **233**, 363.
8. Kreuer, K. D., Protonic conducting oxides. *Annu. Rev. Mater. Res.*, 2003, **33**, 333.
9. Katahira, K., Kohchi, Y., Shimura, T. and Iwahara, H., Protonic conduction in Zr-substituted $BaCeO_3$. *Solid State Ionics*, 2000, **138**, 91.
10. Cervera, R. B., Oyama, Y., Miyoshi, S., Kobayashi, K., Yagi, T. and Yamaguchi, S., Structural study and proton transport of bulk nanograined Y-doped $BaZrO_3$ oxide protonics materials. *Solid State Ionics*, 2008, **179**, 236.
11. Yamada, M., Wei, M., Honma, I. and Zhou, H., One-dimensional proton conductor under high vapor pressure condition employing titanate nanotube. *Electrochem. Commun.*, 2006, **8**, 1549.
12. Park, H. J. and Kim, S., The Grain boundary conduction in Sr-doped lanthanum gallates: a quantitative analysis on the space charge effects. *J. Phys. Chem. C*, 2007, **111**, 14903.
13. Kim, S. and Maier, J., On the conductivity mechanism of nanocrystalline ceria. *J. Electrochem. Soc.*, 2002, **149**, J73.
14. Kreuer, K. D., Proton conductivity: materials and applications. *Chem. Mater.*, 1996, **8**, 610.
15. Norby, T., Solid-state protonic conductors: principles, properties, progress and prospects. *Solid State Ionics*, 1999, **125**, 1.
16. Kreuer, K. D., Adams, S., Münch, W., Fuchs, A., Klock, U. and Maier, J., Proton conducting alkaline earth zirconates and titanates for high drain electrochemical applications. *Solid State Ionics*, 2001, **145**, 295.
17. Tuller, H. L., Ionic conduction in nanocrystalline materials. *Solid State Ionics*, 2000, **131**, 143.
18. Kreuer, K. D., Aspects of the formation and mobility of protonic charge carriers and the stability of perovskite-type oxides. *Solid State Ionics*, 1999, **125**, 285.
19. Shi, C., Yoshino, M. and Morinaga, M., First-principles study of protonic conduction in In-doped $AZrO_3$ (A = Ca, Sr Ba). *Solid State Ionics*, 2005(176), 1091.
20. Atkinson, A., Grain-boundary diffusion: an historical perspective. *J. Chem. Soc. Faraday Trans.*, 1990, **86**, 1307.
21. Wuensch, B. J. and Tuller, H. L., Lattice diffusion, grain boundary diffusion and defect structure of ZnO. *J. Phys. Chem. Solids*, 1994, **55**, 975.
22. Merkle, K. L. and Thompson, L. J., High-resolution electron microscopy of twist and general grain boundaries. *Phys. Rev. Lett.*, 1999, **83**, 556–559.
23. Atkinson, A., Diffusion along grain boundaries and dislocations in oxides, alkali halides and carbides. *Solid State Ionics*, 1984, **12**, 309.
24. Zhu, J. X., Zhou, D. F., Guo, S. R., Ye, J. F., Hao, X. F., Cao, X. Q. *et al.*, Grain boundary conductivity of high purity neodymium-doped ceria nanosystem with and without the doping of molybdenum oxide. *J. Power Sources*, 2007, **174**, 114.
25. Tao, S. and Irvine, T. S., Conductivity studies of dense yttrium-doped $BaZrO_3$ sintered at 1325 °C. *J. Solid State Chem.*, 2007, **180**, 3493.
26. Maier, J., Ionic conduction in space charge regions. *Prog. Solid State Chem.*, 1995, **23**, 171.
27. Maier, J., On the conductivity of polycrystalline materials. *Ber. Bunsenges Phys. Chem.*, 1986, **90**, 26.
28. Maier, J., Space charge regions in solid two phase systems and their conduction contribution. I. conductance enhancement in the system ionic conductor-'inert' phase and application on $AgCl{:}Al_2O_3$ and $AgCl{:}SiO_2$. *J. Phys. Chem. Solids*, 1985, **46**, 309.
29. Kliewer, K. L. and Koehler, J., Space charge in ionic crystals. *Phys. Rev. A*, 1965, **140**, 1126.
30. Guo, X. and Waser, R., Electrical properties of the grain boundaries of oxygen ion conductors: acceptor-doped zirconia and ceria. *Prog. Mater. Sci.*, 2006, **51**, 151.
31. Stotz, S. and Wagner, C., Solubility of water vapor and hydrogen in solid oxides. *Ber. Bunsen-Ges. Phy. Chem.*, 1966, **70**, 781.

32. Kreuer, K. D., SchÖnherr, E. and Maier, J., Proton and oxygen diffusion in $BaCeO_3$ based compounds: a combined thermal gravimetric analysis and conductivity study. *Solid State Ionics*, 1994, **70/71**, 278.
33. Kreuer, K. D., Dippel, T., Baikov, Y. M. and Maier, J., Water solubility, proton and oxygen diffusion in acceptor doped $BaCeO_3$: a single crystal analysis. *Solid State Ionics*, 1996, **86/88**, 613.
34. Müller, J., Kreuer, K. D., Maier, J., Matsuo, S. and Ishigame, M., A conductivity and thermal gravimetric analysis of a Y-doped $SrZrO_3$ single-crystal. *Solid State Ionics*, 1997, **97**, 421.
35. Iguchi, F., Sata, N., Tsurui, T. and Yugami, H., Microstructures and grain boundary conductivity of $BaZr_{1-x}Y_xO_3$ ($x = 0.05$, 0.10, 0.15) ceramics. *Solid State Ionics*, 2007, **178**, 691.
36. Bohn, H. G. and Schober, T., Electrical conductivity of the high-temperature proton conductor $BaZr_{0.9}Y_{0.1}O_{2.95}$. *J. Am. Ceram. Soc.*, 2000, **83**, 768.
37. Schober, T. and Bohn, H. G., Water vapor solubility and electrochemical characterization of the high temperature proton conductor $BaZr_{0.9}Y_{0.1}O_{2.95}$. *Solid State Ionics*, 2000, **127**, 351.
38. Slade, R. C. T., Flint, S. D. and Singh, N., Investigation of protonic conduction in Yb- and Y-doped barium zirconates. *Solid State Ionics*, 1995, **82**, 135.
39. Snijkers, F. M. M., Buekenhoudt, A., Cooymans, J. and Luyten, J. J., Proton conductivity and phase composition in $BaZr_{0.9}Y_{0.1}O_3$. *Scripta Mater.*, 2004, **50**, 655.
40. Baik, H. D., Proton conduction in Y_2O_3-doped $SrZrO_3$. *J. Korean Ceram. Soc.*, 2002, **39**, 635.
41. Münch, W., Kreuer, K. D., Seifert, G. and Maier, J., Proton diffusion in perovskites: comparison between $BaCeO_3$, $BaZrO_3$, $SrTiO_3$, and $CaTiO_3$ using quantum molecular dynamics. *Solid State Ionics*, 2000, **136–137**, 183.
42. Ryu, K. H. and Haile, S. M., Chemical stability and proton conductivity of doped $BaCeO_3$–$BaZrO_3$ solid solutions. *Solid State Ionics*, 1999, **125**, 355.
43. Potter, A. R. and Baker, R. T., Impedance studies on $Pt|SrCe_{0.95}Yb_{0.05}O_3|Pt$ under dried and humidified air, argon and hydrogen. *Solid State Ionics*, 2006, **177**, 1917.
44. Sammes, N., Phillips, R. and Smirnova, A., Proton conductivity in stoichiometric and sub-stoichiometric yittrium doped $SrCeO_3$ ceramic electrolytes. *J. Power Sources*, 2004, **134**, 153.
45. Azad, A. K. and Irvine, J. T. S., Synthesis, chemical stability and proton conductivity of the perovksites $Ba(Ce\,Zr)_{1-x}Sc_xO_3$. *Solid State Ionics*, 2007, **178**, 635.
46. Murugaraj, P., He, T., Schober, T. and Maier, J., High proton conductivity in barium yttrium stannate $Ba_2YSnO_{5.5}$. *Solid State Ionics*, 1997, **98**, 1.
47. Zhang, G. B. and Smyth, D. M., Protonic conduction in $Ba_2In_2O_5$. *Solid State Ionics*, 1995, **82**, 153.
48. Hui, R., Maric, R., Petit, C. D., Styles, E., Qu, W., Zhang, X. *et al.*, Proton conduction in ceria-doped $Ba_2In_2O_5$ nanocrystalline ceramic at low temperature. *J. Power Sources*, 2006, **161**, 40.
49. Bohn, H. G., Schober, T., Mono, T. and Schilling, W., The high temperature proton conductor $Ba_3Ca_{1.18}Nb_{1.82}O_9$. I. Electrical conductivity. *Solid State Ionics*, 1999, **117**, 219.
50. Corcoran, D. J. D. and Irvine, J. T. S., Investigations into $Sr_3CaZr_{0.5}Ta_{1.5}O_{8.75}$, a novel proton conducting perovskite oxide. *Solid State Ionics*, 2001, **145**, 307.
51. Savanju, C. and Irvine, J. T. S., $Sr_3Ca_{1-x}Zn_xZr_{0.5}Ta_{1.5}O_{8.75}$: a study of the influence of the B-site dopant nature upon protonic conduction. *Solid State Ionics*, 2003, **162/163**, 105.
52. Norby, T., Dyrlie, O. and Kofstad, P., Protons in Ca-doped La_2O_3 and $LaNdO_3$. *Solid State Ionics*, 1992, **53/56**, 446.
53. Norby, T. and Kofstad, P., Direct-current conductivity of Y_2O_3 as a function of water vapor pressure. *J. Am. Ceram. Soc.*, 1986, **69**, 780.
54. Omata, T., Okuda, K., Tsugimoto, S. and Otsuka-Matsuo-Yao, S., Water and hydrogen evolution properties and protonic conducting behaviors of Ca^{2+}-doped $La_2Zr_2O_7$ with a pyrochlore structure. *Solid State Ionics*, 1997, **104**, 249.
55. Ahmed, I., Eriksson, S. G., Ahlberg, E. and Knee, C. S., Influence of microstructure on electrical properties in $BaZr_{0.5}In_{0.5}O_3$ proton conductor. *Solid State Ionics*, 2008, **179**, 15.
56. Badwal, S. P. S., Grain boundary resistivity in zirconia-based materials: effect of sintering temperatures and impurities. *Solid State Ionics*, 1995, **76**, 67.
57. Münch, W., Kreuer, K. D., Seifertli, G. and Maier, J., A quantum molecular dynamics study of proton diffusion in $SrTiO_3$ and $CaTiO_3$. *Solid State Ionics*, 1999, **125**, 39.
58. Kreuer, K. D., On the development of proton conducting materials for technological applications. *Solid State Ionics*, 1997, **97**, 1.
59. Mondal, P., Klein, A., Jaegermann, W. and Hahn, H., Enhanced specific grain boundary conductivity in nanocrystalline Y_2O_3-stabilized zirconia. *Solid State Ionics*, 1999, **118**, 331.
60. Kosacki, I., Rouleau, C. M., Becher, P. F., Bentley, J. and Lowndes, D. H., Nanoscale effects on the ionic conductivity in highly textured YSZ thin films. *Solid State Ionics*, 2005, **176**, 1319.
61. Maier, J., Point-defect thermodynamics and size effects. *Solid State Ionics*, 2000, **131**, 13.
62. Kosacki, I., Anderson, H. U., Mitzutani, Y. and Ukai, K., Nonstoichiometry and electrical transport in Sc-doped zirconia. *Solid State Ionics*, 2002, **152/153**, 431.
63. Ma, X., Dai, J., Zhang, H. and Reisner, D. E., Protonic conductivity nanostructured ceramic film with improved resistance to carbon dioxide at elevated temperatures. *Surf. Coat. Technol.*, 2005, **200**, 1252.
64. Guo, X., On the degradation of zirconia ceramics during low-temperature annealing in water or water vapor. *J. Phys. Chem. Solids*, 1999, **60**, 539.
65. Anselmi-Tamburini, U., Maglia, F., Chiodelli, G., Riello, P., Bucella, S. and Munir, Z. A., Enhanced low-temperature protonic conductivity in fully dense nanometric cubic zirconia. *Appl. Phys. Lett.*, 2006, **89**, 163116.
66. Kim, S., Anselmi-Tamburini, U., Park, H. J., Martin, M. and Munir, Z. H., Unprecedented low-temperature electrical power generation using nanoscale fluorite-structured oxide electrolytes. *Adv. Mater.*, 2008, **20**, 556.
67. Raz, S., Sasaki, K., Maier, J. and Riess, I., Characterization of adsorbed water layers on Y_2O_3-doped ZrO_2. *Solid State Ionics*, 2001, **143**, 181.
68. Contescu, C., Contescu, A. and Schwarz, J. A., Thermodynamics of proton binding at the alumina/aqueous solution interface. A phenomenological approach. *J. Phys. Chem.*, 1994, **98**, 4327.
69. Morimoto, T., Nagao, M. and Tokuda, F., Relation between the amounts of chemisorbed and physisorbed water on metal oxides. *J. Phys. Chem.*, 1969, **78**, 243.
70. Anderson, J. H. and Parks, G. A., Electrical conductivity of silica gel in the presence of adsorbed water. *J. Phys. Chem.*, 1968, **72**, 3662.
71. Krebs, V. B., Die Kristallstruktur von $MoO_3 \cdot 2H_2O$. *Acta Cryst.*, 1972, **B28**, 2222.
72. Li, Y. M., Hibino, M., Miyayania, M. and Kudo, T., Proton conductivity of tungsten trioxide hydrates at intermediate temperature. *Solid State Ionics*, 2000, **134**, 271.
73. Liang, C., Conduction characteristics of the lithium iodide–aluminum oxide solid electrolytes. *J. Electrochem. Soc.*, 1973, **120**, 1289.
74. Varanasi, C., Juneja, C., Chen, C. and Kumar, B., Electrical conductivity enhancement in heterogeneously doped scandia-stabilized zirconia. *J. Power Sources*, 2005, **147**, 128.
75. Beniere, F. and Reddy, K. V., Enhanced ionic transport in NaCl–Al_2O_3 heterogeneous electrolytes. *J. Phys. Chem. Sol.*, 1999, **60**, 839.
76. Kumar, B., Chen, C. and Varanasi, C., Electrical properties of heterogeneously doped yttria stabilized zirconia. *J. Power Sources*, 2005, **140**, 12.
77. Sata, N., Eberman, K., Eberl, K. and Maier, J., Mesoscopic fast ion conduction in nanometre-scale planar heterostructures. *Nature*, 2000, **408**, 946.
78. Azad, S., Marina, O. A., Wang, C. M., Saraf, L., Sutthanandan, V., McCready, D. E. *et al.*, Nanoscale effects on ion conductance of layer-by-layer structures of gadolinia-doped ceria and zirconia. *Appl. Phys. Lett.*, 2005, **86**, 131906.
79. Ponomareva, V. G., Uvarov, N. F., Lavrova, G. V. and Hairetdinov, E. F., Composite protonic solid electrolytes in the $CsHSO_4$–SiO_2 system. *Solid State Ionics*, 1996, **90**, 161.
80. Ponomareva, V. G. and Lavrova, G. V., Influence of dispersed TiO_2 on protonic conductivity of $CsHSO_4$. *Solid State Ionics*, 1998, **106**, 137.

81. Ponomareva, V. G., Merinov, B. V. and Dolbinina, V. V., Composite protonic electrolytes in the system $(NH_4)_3H(SO_4)_2$–SiO_2. *Solid State Ionics*, 2001, **145**, 205.
82. Lavrova, G. V. and Ponomareva, V. G., Intermediate-temperature composite proton electrolyte $CsH_5(PO_4)_2/SiO_2$: transport properties versus oxide characteristic. *Solid State Ionics*, 2008, **179**, 1170.
83. Suksamai, W. and Metcalfe, I. S., Measurement of proton and oxide ion fluxes in a working Y-doped $BaCeO_3$ SOFC. *Solid State Ionics*, 2007, **178**, 627.
84. Kim, S., Lee, K. H. and Lee, H. L., Proton conduction in $La_{0.6}Ba_{0.4}ScO_{2.8}$ cubic perovskite. *Solid State Ionics*, 2001, **144**, 109.